Case Studies in Thermal Engineering 73 (2025) 106554

Contents lists available at ScienceDirect

Case Studies in Thermal Engineering

journal homepage: www.elsevier.com/locate/csite

A new experimental approach to lithium-ion battery fires in electric vehicles: Investigation of fire behavior and effectiveness of extinguishing agents

Onur Mammacıoğlu [a], Gokhan Coskun [a,b,c,*]

[a] Department of Fire and Fire Safety, Sakarya University, Sakarya, Turkey
[b] Department of Mechanical Engineering, Sakarya University, Sakarya, Turkey
[c] Fire Application and Research Center, Sakarya University, Sakarya, Turkey

ARTICLE INFO

Keywords:
Lithium-ion battery fire
Fire extinguisher
Fire experiments

ABSTRACT

This study investigates fire incidents in lithium-ion batteries used in electric vehicles and evaluates the effectiveness of extinguishing agents under controlled conditions, highlighting the difficulty of extinguishing such fires due to the materials in the lithium-based battery components. The combustion of 18,650 Lithium Nickel Manganese Cobalt Oxide (NMC) batteries was initiated using an overheating method in a specialized safety setup. The extinguishing agents tested include Water, BIOVERSAL, NOVEC 1230, and COG (high-viscosity liquid substance). The first phase involved a single-battery combustion test, followed by intervention tests under two conditions, which were the heat supply cut off and continuous heat application. Performance was evaluated based on combustion and explosion temperatures, ignition delay, and variations in ambient gas composition (O_2, CO, CO_2). Under heat-cut conditions, BIOVERSAL exhibited superior thermal resistance (~247,6 °C), while Water provided a longer ignition delay of about 82 s. In continuous heat conditions, COG achieved the highest explosion temperature (~247 °C) and longest ignition delay about 75 s, significantly outperforming NOVEC 1230, which showed the lowest suppression efficiency. In conclusion, BIOVERSAL and COG were the most effective extinguishing agents, with BIOVERSAL excelling under heat-cut conditions and COG proving most efficient under continuous heat exposure.

1. Introduction

Lithium-ion batteries have become the predominant technology for powering our increasingly portable and mobile world. Their high energy density—enabling substantial energy storage in a compact form factor—coupled with the capacity for hundreds of recharges cycles, makes them ideally suited for a broad range of applications. As a result, energy storage using lithium-ion batteries (LIBs) has emerged as a key trend across various industries. LIBs have emerged as promising energy storage devices and have become ubiquitous in the field of consumer electronics, electrochemical energy storage stations (ESS) and electric vehicles (EVs) due to their high energy density, extended cycle life and high operating potential [1]. LIBs are widely used in electrochemical energy storage but contain reactive and flammable materials [2]. Lithium-ion batteries (LIBs) are susceptible to thermal runaway (TR), a phenomenon

* Corresponding author. Department of Mechanical Engineering, Sakarya University, Sakarya, Turkey.
E-mail address: gcoskun@sakarya.edu.tr (G. Coskun).

https://doi.org/10.1016/j.csite.2025.106554
Received 16 February 2025; Received in revised form 4 May 2025; Accepted 22 June 2025
Available online 23 June 2025

that often culminates in fire through a chemical process. Although the chain of chemical reactions in LIB fires resembles that of a standard fire tetrahedron, LIB fires are particularly challenging to extinguish using conventional extinguishing agents. The failures of LIBs may be triggered when the battery is exposed to an abnormal operating environment, such as mechanical damage, external short circuit, over-charge and over-discharge as well as the external heating [2]. These failures, like other fires, result in the release of smoke and flames. However, unlike typical fires, lithium-ion battery fires can exhibit characteristics of nearly all fire classes, making them more complex and hazardous to manage. The combustible materials in the process of TR of LIB consist of graphite anode (flammable solid material), organic electrolyte (flammable liquid), combustible gas (flammable gas) and lithium metal (combustible metal). In addition, the composition of combustible materials is also changing in the process of TR [1].

LIBs fire has a large heat release rate, a fast temperature rise rate and a long-elevated temperature duration [1]. Overheating of the batteries may result in exothermal reactions and lead to a thermal runaway with excessive amounts of heat, gas emissions, fire and potentially explosion/rapid dissembling. Even if there is no thermal runaway, a heated battery can still vent flammable and toxic gases. Examples of toxic gases that may originate from such events are hydrogen fluoride (HF) and phosphorous oxyfluoride (POF3) [3]. The susceptibility of LIBs to fire and explosion under harsh conditions (overheating, overcharging, crushing, puncturing, water immersion, short-circuiting etc.), which could be attributed to their unique chemical composition, stored electrical energy, and construction, has become a significant challenge [1]. Abuse conditions like puncture, overheating and overcharge can cause heat accumulation inside Li-ion battery due to a series of exothermic reactions. Heat accumulation can elevate the cell temperature and accelerate the exothermic reaction in return, which possibly lead to thermal runaway (TR) behavior [5]. The activity of cathode material, discharging rates, even battery shape was also found to influence the criticality of battery TR [5]. LIBs fire has a large heat release rate, a fast temperature rise rate and a long-elevated temperature duration [1]. The hazardous effects of li-ion battery of TR is strongly depended on state of charge (SOC). The normalized HRR value for the full charged batteries is slightly lower than that of gasoline [5].

The propensity of lithium-ion batteries to catch fire has highlighted the necessity for manufacturers to enhance their safety. In this regard, various methods are employed to improve the thermal safety of batteries, including air cooling, liquid cooling, phase change materials, heat pipe cooling, and hybrid thermal management strategies. Additionally, safer design practices are being implemented, such as the use of more reliable separators, non-flammable liquid electrolytes, lithium dendrite-free anodes, and thermally stable cathodes. These advancements aim to mitigate the risks associated with thermal runaway and improve overall battery safety. LIB fires still occur frequently, and each occurrence is usually accompanied by explosion and toxic gas, which pose an acute threat to human safety [1]. The propagation characters for LIB arrays at different SOCs were different [4] and the mass loss process and HRR were mainly depending on SOC [6]. As the SOC level increases, the probability of a fire also increases. When you look at the changes of cell temperature, HRR, toxic gases concentration, and voltage under a controlled propane fire; 100 % SOC LIB cell reactions were more intense than the lower SOC one when exposed to fire [6].

The initiation of lithium-ion battery (LIB) fires can be effectively illustrated using the LIB fire triangle, analogous to the basic description of the combustion reaction. This model demonstrates that, in addition to the traditional combination of flammable material, heat, and oxygen—key components in fire suppression—the chain effect of chemical reactions also occurs spontaneously in LIB fires. As depicted in Fig. 1, air or oxygen released by the cathode serves as the oxidizing agent, while the organic electrolyte or flammable gases act as the flammable materials. Abuse conditions, such as mechanical, electrical, or thermal abuse, function as the primary heat sources that trigger the combustion process.

During the initial stage of exothermic reaction, the solid electrolyte interphase (SEI) layer firstly decomposes at 90°C-120 °C, causing the anode to be exposed to the electrolyte [7]. Without the protection of the SEI layer, the graphite anode will react with electrolyte [8]. Further, the separator inside the battery will melt when the temperature exceeds around 130 °C, resulting in micro inner short circuit inside the cell [9]. The micro inner short circuit could transform the electric energy stored in the battery to joule heat and further accelerate the temperature rise of the battery [10,11]. As the temperature increases, the separator continues to melt or even collapse, resulting in the large-scale short circuit and joule heat accumulation inside the battery [12]. Subsequently, the cathode, anode and electrolyte inside the battery decomposes drastically when the temperature exceeds around 200 °C [13]. Then, the temperature increases exponentially, and the battery becomes an ignition source. The anode, cathode, separator and electrolyte inside the battery are all flammable materials. In addition, the reaction mentioned above will also produce some combustible gases, such as H_2, CH_4, C_2H_4 and C_2H_6 [14].

The oxidant is not only provided by air, but also the oxygen generated by the cathode decomposition [15,16]. When evaluating

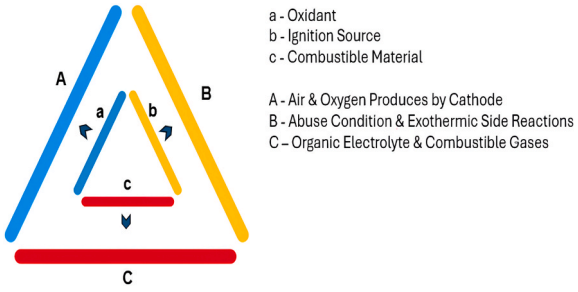

Fig. 1. LIB fire triangle [1].

battery safety using gas flammability limits, two key indicators are considered: the lower flammability limit and the range of flammable concentrations. A lower flammability limit and a wider range of flammable concentrations increase the likelihood of mixed gases meeting combustion conditions, thereby posing a greater explosion hazard [17]. In general, the combustion characters of LIBs can be summarized into the four stages: ignition, fierce ejection (Jet fire), combustion, weakening and extinguishment [18]. In lithium-ion batteries (LIBs), which undergo decomposition at high temperatures, a phenomenon known as jet fire occurs around 176 °C–230 °C. Jet fire refers to the combustion of decomposed substances within the battery when the safety valve opens. The safety valve is designed to regulate the internal pressure of the battery, preventing simultaneous combustion of the entire battery; however, it also triggers a burning effect like a jet flame, resembling that seen in jet engines. Following a jet fire, heat transfer accelerates, pushing neighboring batteries that have not yet reached the jet fire stage towards this phase. Batteries that have reached the jet fire stage immediately enter complete combustion, although the flames appear calmer compared to the initial jet fire. Once this combustion phase concludes, the flames begin to subside as the available flammable materials and oxygen are depleted. All stages are illustrated in Fig. 2.

Fire-extinguishing agents are utilized to suppress burning materials by absorbing heat, removing oxygen, and disrupting the chemical reaction chain. However, LIB fires exhibit combustion phenomena that directly counteract these suppression mechanisms, making the suppression of LIB fires particularly challenging. Currently, the extinguishing agents used for LIB fires are classified into solid, liquid and gaseous extinguishing agents. Each type has distinct advantages, disadvantages, extinguishing mechanisms, and suitable application scenarios. Li et al. [19] found that when ABC dry chemical powder was applied to extinguish an LCO battery fire, re-ignition occurred 8 s after the visible flame was suppressed. They also observed that dry chemical powder leaves significant residue after application, making cleanup difficult. If not cleaned promptly, the residual powder can absorb moisture, become electrically conductive, and potentially cause external short circuits in the battery cells. Therefore, dry powder is not considered suitable for extinguishing LIB fires.

Xu et al. [20] demonstrated that the use of water mist is effective in preventing thermal runaway and cooling the battery. Additionally, it was determined that extending the duration of water mist application can further delay the onset of thermal runaway propagation and ultimately restrain its spread. However, Zhang et al. [21] reported that water mist struggled to extinguish a battery fire with a capacity of 243 Ah, and that the heat release rate of the cell increased during the application of water mist, while the total heat release was similar to the case without any extinguishing agent. Furthermore, it was noted that due to the influence of ventilation and obstacles, water mist particles have difficulty reaching the battery surface. Larsson et al. [3] also found that the use of water mist increases the production of hydrogen fluoride. Therefore, the risk of increased toxicity during firefighting must be carefully considered.

According to the study conducted by Peng et al. [22], in order to enhance the fire-extinguishing performance of water mist for lithium-ion battery fires, three types of nonionic surfactants (FS3100, Tween 80, and APG0810) were compared. APG0810 improves the cooling and extinguishing capabilities of water mist by effectively reducing the surface tension of water, while Tween 80 enhances fire suppression through its high foaming ability, directly reducing the maximum cell surface temperature during thermal runaway. Although APG0810 demonstrated superior overall cooling performance, it was less effective than Tween 80 in controlling the peak temperature of the battery cells. The addition of defoaming agents to the APG0810 solution increased bubble brittleness and improved the cooling effect on the cell surface, with APG0810-1 showing the most effective performance by simultaneously reducing foam

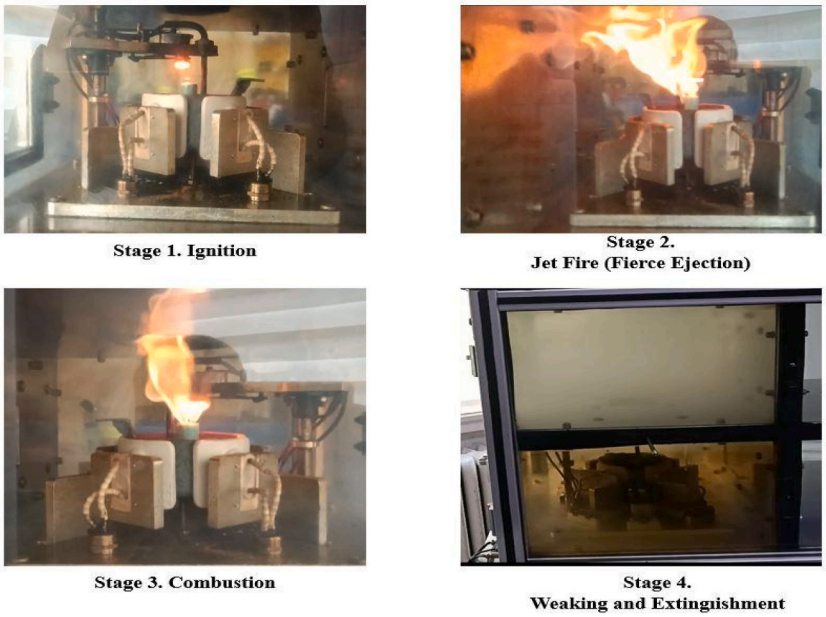

Fig. 2. Stages of LIB fires.

generation and promoting bubble rupture. The findings suggest that formulations with appropriate foam content and brittleness are crucial for effectively mitigating the risk of TR in LIB fires. The addition of F-500 agent has demonstrated the ability to effectively extend the ignition induction time and lower the peak temperature of the LIB flame. Nevertheless, the high electrical conductivity of water continues to limit its broader development and application [23]. CO_2 is used as a fire-extinguishing agent primarily by reducing or displacing oxygen in the environment. The generation of oxygen by LIBs during the combustion process significantly limits the effectiveness of CO_2 as an extinguishing agent. Xu et al. [24] concluded in their study that even if the visible flame is suppressed before the extinguishing agent is deployed, the ignition source and oxidizer are not entirely eliminated, leading to a frequent occurrence of re-ignition when CO_2 is used to suppress LIB fires. Zang et al. [21] found that the use of HFC-227ea exhibited limited effectiveness in extinguishing a 243 Ah large-scale $LiFePO_4$ (LFP) battery fire in an open environment. Therefore, it is recommended that HFC-227ea be applied in confined spaces, deployed as early as possible, and that the cooling time be extended to enhance its extinguishing performance. Zhang et al. [25] found that $C_6F_{12}O$ (NOVEC 1230) exhibited effective fire-extinguishing and cooling performance in a battery module containing 12 LFP LIBs (nominal voltage: 3.7 V, rated capacity: 243 Ah), successfully suppressing the propagation of thermal runaway. However, Liu et al. [26] reported that the use of $C_6F_{12}O$ increases the emission of harmful gases, and that the concentration of these hazardous gases rises with the increasing dosage of $C_6F_{12}O$. Huang et al. [27] identified that the cooling effect of liquid nitrogen on lithium-ion batteries (LIBs) is significantly superior to that of other gaseous fire-extinguishing agents, capable of reducing the cell surface temperature below 0 °C. Furthermore, liquid nitrogen can delay or even prevent thermal runaway before the cell surface reaches the critical thermal runaway suppression temperature. Therefore, liquid nitrogen is considered to have great potential for fire-extinguishing and rescue operations in LIB fire incidents. However, challenges related to the storage and transportation of liquid nitrogen remain significant obstacles to its practical application. Rao et al. [28] found that aerosol fire-extinguishing agents provide some initial cooling but are unable to significantly reduce the battery temperature until the exothermic reactions within the cell begin to decay. Consequently, the problem of re-ignition remains a major challenge, as a thermally runaway cell can remain hot enough to ignite residual fuel and even trigger thermal runaway in adjacent cells. Furthermore, since the residual aerosol products after water absorption may be corrosive and electrically conductive, they can cause battery damage and even external short circuits. Therefore, it is necessary to promptly clean the protected zone after the application of aerosol fire-extinguishing agents. As a result, aerosol fire-extinguishing agents fail to meet the requirements for effectively suppressing LIB fires.

In this study, it is aimed to develop a fire-extinguishing agent that combines the advantageous properties of existing agents reported in the literature while minimizing their disadvantages, offering high thermal resistance, preventing heat transfer to adjacent cells, and ensuring low toxicity. For this purpose, the overheating period experienced by the battery was analyzed under two main scenarios. The first scenario involved simulating the temperature increase of the battery after being exposed to heat for a specific duration (7 min) and experimentally investigating the effectiveness of water and BIOVERSAL extinguishing agents. The second scenario simulated a continuous exposure to heat, where the situation could not be detected, and experimentally assessed the effectiveness of NOVEC 1230 and COG extinguishing agents. Throughout the experimental procedures, the temperature variations within the battery, the analysis of ambient gases (O_2, CO, CO_2), and the time until explosion or ignition were compared. Within this framework, the study aims to provide a novel perspective to the literature by comparing the use of different extinguishing agents under varying scenarios.

2. Experiments of lithium-ion battery fires

Experimental investigations involving lithium-ion batteries present substantial risks and are associated with inherently hazardous conditions. Consequently, the implementation and consistent utilization of personal protective equipment (PPE) are imperative to ensure safety during experimental procedures and data acquisition processes. The experimental setup is designed to enable combustion in a single cell within a confined space and to monitor its spread across different compartments, allowing for the study of multiple scenarios. This setup replicates the conditions that lead to lithium-ion battery combustion. For this purpose, heat transfer methods (conduction, convection, and radiation) can be applied individually or in combination. The experiments are organized into two main sections. In the first section, the combustion products and temperature fluctuations resulting from battery combustion are analyzed. In the second section, the battery's responses to different fire-extinguishing agents following thermal runaway are investigated. Experiments are outlined in Table 1.

Table 1
Experiment roadmap.

Stages/Expirement Number		Expirement Explanation	3.6 V 3200 mAh NMC Single Li-on Battery
STAGE 1	1	The time at which flaming combustion begins	X
	2	Graph of temperature rise during combustion	X
		Measurement of CO and CO_2 emissions during combustion	
		Monitoring ambient O_2 levels during combustion	
STAGE 2	3	The application of Water as an extinguishing agent	X
	4	The application of NOVEC 1230 as an extinguishing agent	X
	5	The application of BIOVERSAL as an extinguishing agent	X
	6	The application of a High-Viscosity Liquid Substance (COG) as an extinguishing agent	X

2.1. Experimental setup

The entire experimental setup depicted in Fig. 3 is constructed from heat- and explosion-resistant tempered glass and steel. The configuration comprises four cubic chambers. In a cubic chamber, the height (a) of the experimental area is 20 cm, the width (b) is 30 cm, and the depth (c) is 50 cm. The cylindrical container housing the batteries is fabricated from steel. High-resolution camera recordings can be safely captured from outside the tempered glass enclosure. The experimental setup accommodates the application of all heat transfer methods, allowing combustion to be initiated using one or more desired methods. Furthermore, the setup includes a control panel equipped with a recording feature that facilitates real-time monitoring of internal temperature. The areas labeled "window" in the diagram consist of tempered glass windows, which enable the transfer of gases emitted from lithium battery fires to an upper or side compartment, thereby allowing for the safe determination and measurement of gas concentrations.

In addition, the tempered glass windows facilitate the safe application of single or combined fire extinguishing agents before, during, or after thermal runaway events in lithium-ion battery fires. The experimental setup is equipped with 150 W resistance and arc heaters powered by electrical energy, allowing for the simultaneous or separate application of heat treatments.

A temperature measuring device is incorporated to monitor ambient temperature and transmit this data to the control panel. The control panel can record incoming temperature measurements along with time data. Additionally, it enables the gradual adjustment of the heating elements to a specified percentage for precise heat treatment applications. While the ambient temperature was measured using the experimental setup, the temperature of the battery cell was recorded with a Cem DT-3891G 4-Channel Thermocouple Temperature Data Logger, and gas data was collected using the Testo 330 LL. Photographs were taken with a GoPro Hero 7, and thermal images were captured using an Uni-T UTI730E professional thermal camera. A portable smoke fan, powered by an external 220 V source, is included to effectively remove accumulated smoke and explosive vapors from the experimental setup when necessary. Additional safety measures may be implemented during experiments to ensure that data collection and recording occur in a secure working environment. The devices used in the experimental setup and the uncertainty values in the operating range are given in Table 2.

2.2. Experimental procedure

An action camera was utilized to document the various stages of the experimental setup, while a temperature recorder and thermal camera were employed to monitor the heat generated during the experiments on a compartmental basis. A portable multi-gas analyzer and a flue gas measuring device were prepared to detect gases emitted during thermal runaway and combustion products present in the smoke. For the experiments, cylindrical 18,650 model lithium-ion batteries with a nominal voltage of 3.6 V and a capacity of 3200 mAh, specifically Lithium Nickel Manganese Cobalt Oxide (NMC), were used. These batteries were selected due to their widespread availability, cost-effectiveness, and frequent use in electric and hybrid vehicles globally. Thermal runaway and combustion events were initiated using the heating feature of the battery test setup, employing electric heaters (overheating) to commence the combustion experiment. Although the experimental setup was designed to be explosion-proof and smoke-proof, featuring steel frames, compartments containing the batteries, and external windows, additional safety precautions were taken. Personal protective equipment and closed-circuit breathing apparatuses were utilized throughout the experiments to prevent exposure to potentially toxic gases. Furthermore, a portable fume extractor was made available to facilitate the evacuation of smoke and hazardous gases as necessary.

During the experiment, measurements of oxygen, carbon monoxide and ambient temperature were taken and recorded. The heat and smoke values were documented before and during thermal runaway, as well as the detection of gases in the smoke. The behavior of the lithium battery was monitored until it extinguished naturally, without any intervention. In the second stage of the experiments, the application of extinguishing agents was conducted, and the corresponding data were meticulously recorded. At the conclusion of the experiments, data acquisition and processing were carried out through a systematic approach. First, action camera footage was analyzed to evaluate the effects of the extinguishing agents. Data collected from the portable gas analyzer was meticulously examined to identify variations in gas composition. Additionally, information from the flue gas measuring device was processed and converted into time-based graphs, including a specific graph representing carbon dioxide levels over time. Thermocouple data were utilized to generate a time-based temperature graph, providing insight into the thermal behavior of the system. Finally, thermal camera data were

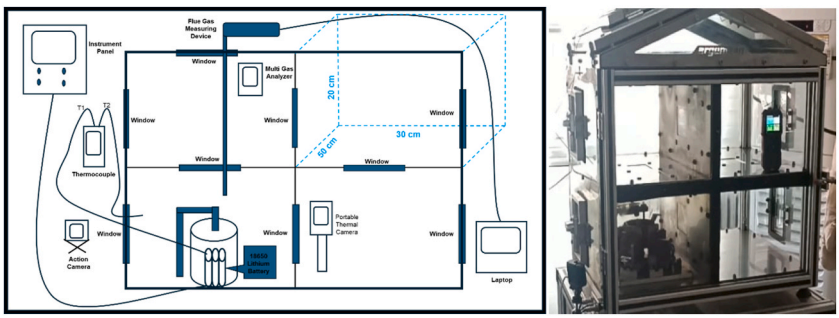

Fig. 3. Expiremental setup.

Table 2
Experimental devices and uncertainty values.

Measured Device	Measured Data	Range	Accuracy
Cem DT-3891G 4-Channel Thermocouple Temperature Data Logger	K type thermocouple	−200 – 1372 °C	±1 °C
Testo 330 LL	O_2	0 to 21 vol%	±0.2 vol%
Testo 330 LL	CO	0–4000 ppm	±20 ppm (0–400 ppm) ±5 % of mv (401–2000 ppm) ±10 % of mv (2001–4000 ppm)
Testo 330 LL	CO_2	0 to 1 vol% 0–10,000 ppm	±75 ppm or ±3 % of mv (0–5000 ppm) ±150 ppm or ±5 % of mv (5001–10,000 ppm)
Uni-T UTI730E Professional Thermal Camera	Thermal image	−40 °C–400 °C	±2 °C or ±2 %

analyzed to assess heat distribution and intensity throughout the experimental process. These steps ensured comprehensive evaluation and interpretation of the experimental results. Each experiment was repeated three times to ensure the accuracy of the experiments.

3. Results and discussion

3.1. Experiment of single battery fire

In the first stage of the experiments, single battery combustion trials (Experiment 1) were conducted. In these trials, the 18,650 model 3.6-V, 3200 mAh NMC lithium battery was heated for 7 min using 150 W of electric energy via conduction. The 7-min duration was selected as a reference because, when exposed to 150 W of energy, the battery typically explodes around the 8th minute. The battery was heated for 7 min to initiate internal decomposition, ensuring that the exothermic reaction would continue independently. At the end of this 7-min period, the temperature of the battery increased from 28.2 °C to 211.9 °C. At this point, heat transfer was halted, and the battery was observed further. It was noted that the exothermic reaction continued, generating heat even after heat treatment ceased. Approximately 1 min and 45 s later, the battery's temperature rose to 212.9 °C. At this stage, a rapid release of gas was observed, followed immediately by explosion and combustion. It was determined that 22 ms elapsed between gas release and explosion. Following the explosion, the temperature surged by 128 °C, reaching 340.9 °C. All data shown in Fig. 4.

Before the explosion, the ambient gas levels were characterized by an oxygen concentration of 21 %, carbon monoxide levels ranging from 0 to 9 ppm, and carbon dioxide levels between 0 and 8 ppm. At the moment of the explosion, the ambient oxygen concentration decreased slightly, ranging between 20 % and 21 %, while carbon monoxide levels increased to a range of 10–41 ppm, and carbon dioxide levels rose to between 9 and 11 ppm. Following the explosion, the ambient oxygen concentration returned to 21 %, whereas carbon monoxide levels exhibited a significant increase, ranging from 41 to 571 ppm. Similarly, carbon dioxide levels experienced a dramatic rise, reaching values between 12 and 972 ppm. Outgassing and Fire shown in.

Fig. 5. These variations highlight the substantial impact of the explosion on the ambient gas composition.

Fig. 6 shows the thermal camera image and data of the battery. In this context; $\mathbf{P_1}$ shows the thermal camera image and data of the battery, 213 °C, $\mathbf{P_2}$ shows the thermal camera image and data of the smoke, 79.1 °C, $\mathbf{P_3}$ shows the thermal camera image and data of the environment, 48.3 °C. Based on the data obtained from the thermal camera image, the center point temperature is 211 °C, the maximum temperature is 361 °C, the minimum temperature is 29.5 °C, and the emissivity is 0.95.

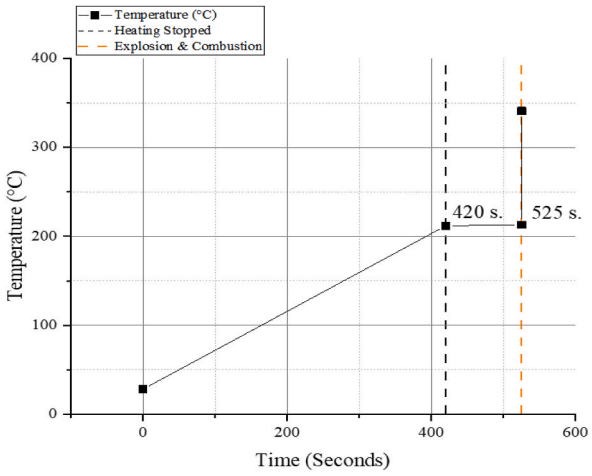

Fig. 4. Battery temperature and critical events.

Fig. 5. Outgassing and fire.

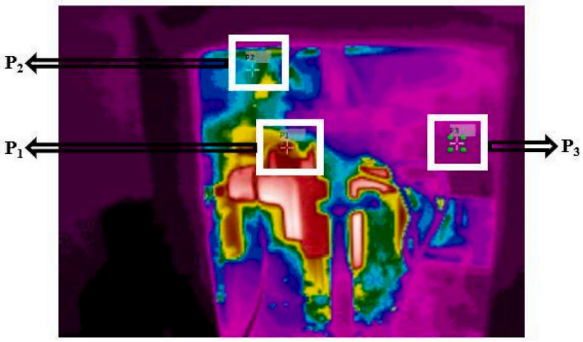

Fig. 6. Thermal camera vision.

3.2. *Experiment of intervention with water on single battery fire*

In the second stage of the experiment, water was applied as an extinguishing agent.

(Experiment 2). In this experiment, the 18,650 model 3.6-V, 3200 mAh NMC lithium battery was heated for 7 min using 150 W of electrical energy via conduction. Following this, the heat supply was halted, and the battery was continuously observed. Since the temperature, CO_2, CO, and O_2 values measured up to this point were like those obtained in Experiment 1, this data was not repeated in this section. After stopping the heat supply, the battery continued its exothermic reaction, resulting in a sustained temperature increase. As the temperature rose, the safety plug released, and immediately after, 5 ml of water was injected into the battery through an intervention apparatus positioned above the battery plug. An explosion and combustion occurred 15 min and 34 s after this intervention. At this stage, the battery's temperature reached approximately 210–215 °C, as in Experiment 1. Following the explosion, the temperature rapidly increased to approximately 311.1 °C. This data is shown in Fig. 7. Intervation with water, outgassing and fire

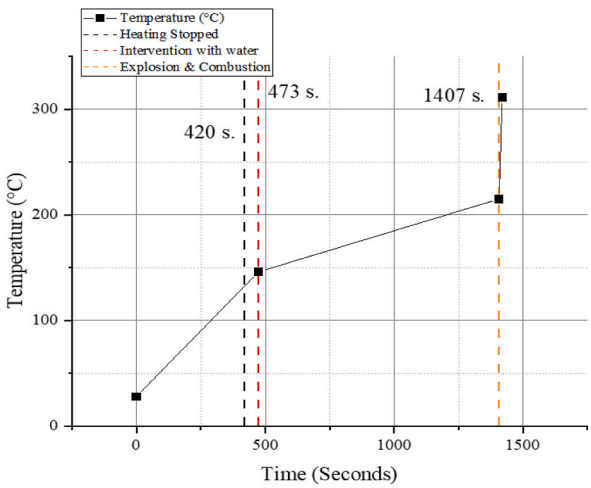

Fig. 7. Battery temperature and critical events (with water).

shown in Fig. 8. According to the obtained data, the use of water as an extinguishing agent demonstrates weak effectiveness in heat absorption. This is due to the high calorific value of the battery, which explains the necessity of using large quantities of water in real-life incidents within this context.

The data obtained from the experiment were systematically analyzed across three primary sections, with the emission data summarized and presented in Table 3.

3.3. Experiment of intervention with NOVEC 1230 on single battery fire

At this stage of the experiment, NOVEC 1230 was tested as an extinguishing agent.

(Experiment 3). Novec 1230 is an environmentally friendly clean agent fire suppression fluid, primarily composed of dodecafluoro-2-methylpentan-3-one, with zero ozone depletion potential and a very low global warming potential. It extinguishes fires by absorbing heat and interrupting the combustion process, making it ideal for use in sensitive environments such as data centers, museums, and medical facilities. In this trial, an 18,650 model 3.6-V, 3200 mAh NMC lithium battery was continuously heated using 150 W of electrical energy by conduction. When foaming was observed at the battery plug during the heating process, 5 ml of NOVEC 1230 extinguishing agent was applied, and the battery was subsequently monitored. Foaming at the battery plug was observed 8 min and 8 s after heating began, at which point the battery's temperature had reached approximately 164.8–180 °C. Following the application of NOVEC 1230, the battery's temperature dropped to around 61.5–100.4 °C within approximately 20 s. However, approximately 81 s after the extinguishing agent was applied, the battery exploded and ignited. During this explosion and combustion process, the battery's temperature ranged from approximately 178.9 °C–349.7 °C, and it continued to burn for approximately 43 s following the explosion. These datas shown in Fig. 9. Intervation with NOVEC 1230, outgassing and fire shown in Fig. 10.

The data obtained from the experiment were systematically analyzed across three primary sections, with the emission data summarized and presented in Table 4.

3.4. Experiment of intervetion with BIOVERSAL on single battery fire

At this stage, the experiment using BIOVERSAL as an extinguishing agent was conducted (Experiment 4). Bioversal is an environmentally friendly fire suppression agent derived from biodegradable plant-based components, designed to combat hydrocarbon-based fires effectively. It works by encapsulating and isolating flammable hydrocarbons, suppressing flames while minimizing environmental impact and toxic residues. In this trial, an 18,650 model 3.6-V, 3200 mAh NMC lithium battery was heated for 7 min using 150 W of electrical energy by conduction, after which the heat supply was halted, and the battery was observed. As the temperature, CO_2, CO, and O_2 values obtained up to this point were similar to those in Experiment 1, these data were not included again here. After stopping the heat supply, the battery continued its exothermic reaction, with a corresponding increase in temperature. As the temperature rose, the safety plug released, at which point 5 ml of BIOVERSAL was injected through an intervention apparatus positioned above the battery plug. The battery temperature had reached approximately 146.3 °C by the time the safety plug was blown. An explosion and combustion occurred 14 min and 12 s after the injection of BIOVERSAL, with the battery's temperature rising to approximately 247.6 °C just before ignition. These datas shown in Fig. 11. Intervation with BIOVERSAL, outgassing and fire shown in Fig. 12.

The data obtained from the experiment were systematically analyzed across three primary sections, with the emission data summarized and presented in Table 5.

3.5. Experiment of intervention with COG on single battery fire

In this stage of the experiment, COG was used as an extinguishing agent (Experiment 5). An 18,650 model 3.6-V, 3200 mAh NMC lithium battery was continuously heated by conduction with 150 W of electrical energy. During the heating process, 10 ml of COG extinguishing agent was applied after the battery's safety plug was released. Observation continued after the application.

Fig. 8. Intervention with water, outgassing and fire.

Table 3
Ambient gas (with water).

Ambient O_2		Ambient CO	Ambient CO_2
Before Intervention	21 %	Between 0 and 10 ppm	Between 0 and 12 ppm
After Intervention (with water)	21 %	First reached 13 ppm from 10, then dropped to 2 ppm, but this situation did not last long, until before the explosion, it reached 37 ppm again	First reach 13 ppm from 12, then drop 10 ppm, but this situation did not last long, until before the explosion, it reached 14 ppm again
After the Explosion	Between 20 and 21 %	Between 37 and 931 ppm	Between 14 and 18 ppm

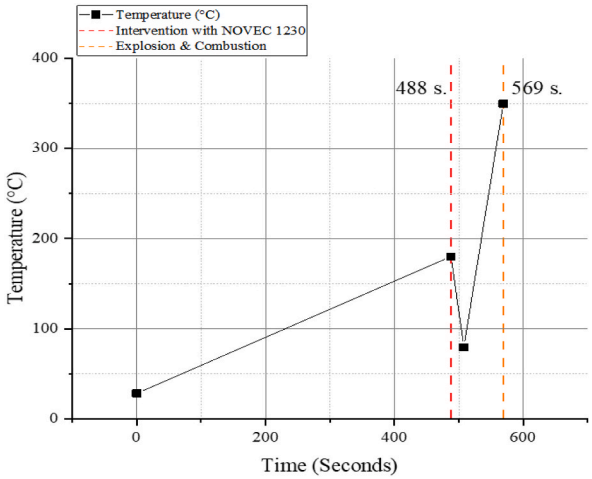

Fig. 9. Battery temperature and critical events (with NOVEC 1230).

Fig. 10. Intervention with NOVEC 1230, outgassing and fire.

Table 4
Ambient gas (with NOVEC 1230).

Ambient O_2		Ambient CO	Ambient CO_2
Before Intervention	21 %	Between 0 and 9 ppm	Between 0 and 11 ppm
After Intervention (with NOVEC 1230)	21 %	Between 9 and 328 ppm	Between 11 and 15 ppm
After the Explosion	Between 17 % and 21 %	Between 328 and 1610 ppm	Between 15 and 37 ppm

Approximately 8 min and 50 s after heating commenced, the battery plug released, and the battery temperature reached around 220 °C. Following the application of COG—approximately 2 s after the plug release—the temperature dropped to approximately 208.5 °C within 11 s, though it then began to rise again. After the gas escape and plug release, the battery was exposed to 10 ml of COG extinguishing agent for 3 min and 36 s, effectively resisting further temperature increase and fire. An increase of ~125 °C was observed in battery temperature at the point of venting and explosion. Following the explosion, the battery continued to burn for approximately 30 s. These datas shown in Fig. 13. Intervation with COG, outgassing and fire shown in Fig. 14.

The data obtained from the experiment were systematically analyzed across three primary sections, with the emission data summarized and presented in Table 6.

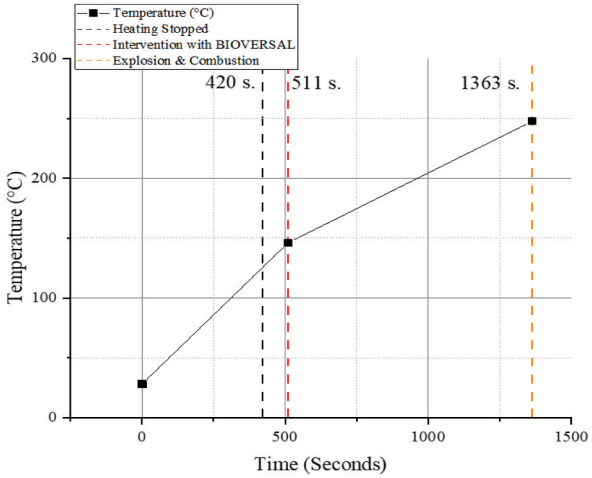

Fig. 11. Battery temperature and critical events (with BIOVERSAL).

Fig. 12. Intervention with BIOVERSAL, outgassing and fire.

Table 5
Ambient gas (with BIOVERSAL).

Ambient O_2		Ambient CO	Ambient CO_2
Before Intervention	21 %	Between 0 and 17 ppm	Between 0 and 10 ppm
After Intervention (with BIOVERSAL)	Between 20 % and 21 %	First slowly drop 17 ppm–2 ppm, but this situation did not last long, until before the explosion, it reached 84 ppm again.	Between 10 and 11 ppm
After the Explosion	Between 20 % and 21 %	Between 200 and 1025 ppm	Between 14 and 18 ppm

3.6. Comparison of all experimental results

In the single-battery combustion test, after the explosion and fire occurred, the ambient measurements were as follows: the O_2 concentration was at 21 %, CO levels ranged from 41 to 571 ppm, and CO_2 levels varied between 12 and 972 ppm. Following the explosion and fire that occurred after water intervention, the O_2 value decreased to between 20 % and 21 %, CO levels increased to a range of 37–931 ppm, while CO_2 levels remained consistent between 14 and 18 ppm. If took place after intervention with NOVEC 1230, the O_2 concentration fell to between 17 % and 21 %, with CO levels recorded between 41 and 571 ppm and CO_2 levels between 15 and 37 ppm. For the explosion and fire event following BIOVERSAL intervention, the O_2 value remained at 20 %–21 %, while CO levels ranged from 200 to 1025 ppm and CO_2 levels were consistent with previous measurements between 14 and 18 ppm. Lastly, in the explosion and fire event that occurred after intervention with COG, the O_2 levels were between 20 % and 21 %, CO concentrations ranged from 24 to 659 ppm, and CO_2 levels again were between 10 and 19 ppm. These data are summarized in Table 7.

When comparing the times taken to reach the temperatures at which fire and explosion occurred, several findings were observed. In the single-battery combustion test, with the heat supply stopped after 7 min from the start, fire and explosion occurred after 8 min and 51 s. When water was used as an intervention, with the heat supply also cut at 7 min, the time to reach fire and explosion temperature extended to 15 min and 34 s. With the NOVEC 1230 intervention, where heat was continuously supplied, the time to reach the critical temperature was 1 min and 21 s. In the experiment with BIOVERSAL, where the heat supply was again cut at 7 min, fire and explosion

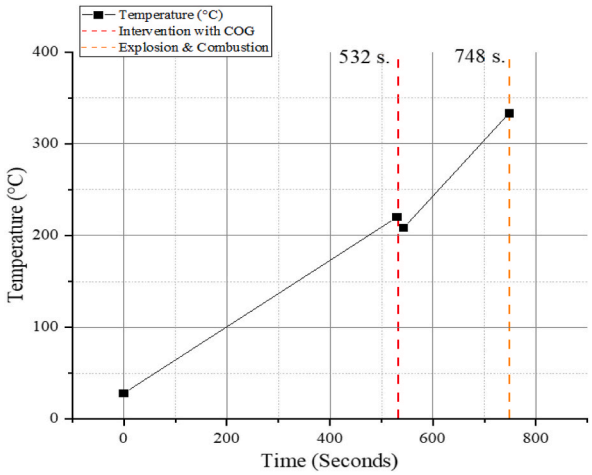

Fig. 13. Battery temperature and critical events (with COG).

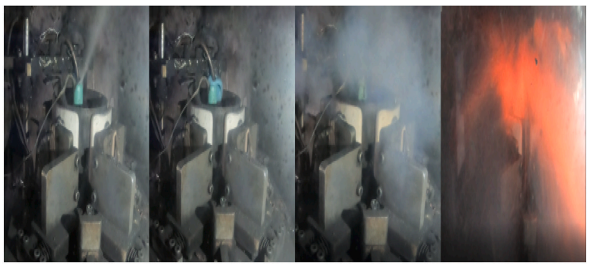

Fig. 14. Outgassing, intervention with COG, pre-fire, and fire.

Table 6
Ambient gas (with COG).

Ambient O_2		Ambient CO	Ambient CO_2
Before Intervention	21 %	Between 0 and 7 ppm	Between 0 and 11 ppm
After Intervention (with COG)	21 %	First slowly drop 7 ppm–3 ppm, but this situation did not last long, until before the explosion, it reached 24 ppm again.	Between 10 and 11 ppm
After the Explosion	Between 20 % and 21 %	Between 24 and 659 ppm	Between 10 and 19 ppm

occurred after 14 min and 12 s. For the COG intervention, conducted with continuous heating, fire and explosion were reached after 3 min and 36 s. These results illustrate how different extinguishing agents and heat application methods impact the time needed to reach temperatures at which fire and explosion are triggered.

4. Conclusion

In these experiments, the first scenario underscores the importance of early intervention, highlighting the critical role that prompt action can play in mitigating fire risks. The second scenario provides insight into the effectiveness of various extinguishing agents in situations where passive systems (such as Battery Management Systems, BMS) fail to prevent overheating of the battery. The cylindrical 18,650 model lithium-ion batteries (3.6 V, 3200 mAh) containing Lithium Nickel Manganese Cobalt Oxide (NMC) were used. A series of extinguishing agents were tested to mitigate the effects of fire when the battery's safety plug was released due to combustion and heat from a single battery. During the trials, when the battery ignited, the temperature over time and levels of O_2, CO_2, and CO gases in the environment were measured. Based on the data obtained, the battery was observed to explode and ignite at approximately 213 °C without intervention, 215 °C when extinguished with water, 236.2 °C with NOVEC 1230, 247.6 °C with BIOVERSAL, and 247 °C with COG extinguishing agent.

These observations underscore the impact of various extinguishing agents and heat application methods on the time needed to reach critical temperatures that can lead to fire and explosion. The test results should be interpreted as two distinct scenarios. In the

Table 7
General results of all experiments.

Experiment	Combustion and Explosion Temperature	Time to Reach Combustion and Explosion Temperature	Time to Reach Combustion and Explosion Temperature after Intervention	Post-Explosion and Post-Combustion Ambient Gases
Single Battery Fire (heat energy was cut off after 7 min at the beginning of the experiment)	~213 °C	8 min 51 sec.	(No intervention)	O_2: 21 %, CO: 41–571 ppm CO_2: 12–972 ppm
Intervention with WATER (heat energy was cut off after 7 min at the beginning of the experiment)	~215 °C	–	15 min 34 sec.	O_2: 20–21 %, CO: 37–931 ppm CO_2: 14–18 ppm
Intervention with NOVEC 1230 (continuous energy was supplied)	~236,2 °C	–	1 min 21 sec. (Beginning of the Exp.Total Time 9 min 29 sec.)	O_2: 17–21 %, CO: 328–1610 ppm CO_2: 15–37 ppm
Intervention with BIOVERSAL (heat energy was cut off after 7 min at the beginning of the experiment)	~247,6 °C	–	14 min 12 s.	O_2: 20–21 %, CO: 200–1025 ppm CO_2: 14–18 ppm
Intervention with COG (continuous energy was supplied)	~247 °C	–	3 min 36 sec. (Beginning of the Exp.Total Time 12 min 25 sec.)	O_2: 20–21 %, CO: 24–659 ppm CO_2: 10–19 ppm

first scenario, energy is supplied solely for the duration necessary to initiate a fire reaction in the battery. In contrast, the second scenario involves continuous exposure of the battery to heat energy. This sustained application of heat energy creates more challenging conditions for the extinguishing agents to function effectively, and this factor should be considered when making comparisons. In all extinguishing agent trials, an increase in gas production was observed during the phases in which the battery was allowed to burn freely. In the evaluation of the first scenario, water and BIOVERSAL demonstrated nearly equivalent performance. Conversely, in the second scenario, the COG extinguishing agent proved to be more effective than NOVEC 1230 in terms of delaying fire. Despite being subjected to heating throughout the experiment, the COG extinguishing agent displayed a notable resistance to both explosion and fire.

CRediT authorship contribution statement

Onur Mammacıoğlu: Writing – original draft, Methodology, Investigation, Data curation, Conceptualization, Validation, Writing – review & editing. **Gokhan Coskun:** Writing – review & editing, Supervision, Investigation, Funding acquisition, Conceptualization, Project administration.

Declaration of competing interest

The authors declare that they have no known competing financial interests or personal relationships that could have appeared to influence the work reported in this paper.

Acknowledgment

This work was supported by Scientific Research Projects Coordinatorship of Sakarya University under grant number 2024-25-59-73.

Data availability

Data will be made available on request.

References

[1] L. Zhang, K. Jin, J. Sun, Q. Wang, A review of fire-extinguishing agents and fire suppression strategies for lithium-ion batteries fire, Fire Technol. 60 (2024) 817–858, https://doi.org/10.1007/S10694-022-01278-3.
[2] Y. Zhang, D. Kong, P. Ping, H. Zhao, X. Dai, X. Chen, Effect of a plate obstacle on fire behavior of 18650 lithium ion battery: an experimental study, J. Energy Storage 54 (2022), https://doi.org/10.1016/j.est.2022.105283.
[3] F. Larsson, P. Andersson, P. Blomqvist, A. Lorén, B.E. Mellander, Characteristics of lithium-ion batteries during fire tests, J. Power Sources 271 (2014) 414–420, https://doi.org/10.1016/j.jpowsour.2014.08.027.
[4] J. Zhao, F. Xue, Y. Fu, Y. Cheng, H. Yang, S. Lu, A comparative study on the thermal runaway inhibition of 18650 lithium-ion batteries by different fire extinguishing agents, iScience 24 (2021), https://doi.org/10.1016/J.ISCI.2021.102854.
[5] P. Huang, H. Chen, A. Verma, Q. Wang, P. Mukherjee, J. Sun, Non-dimensional analysis of the criticality of Li-ion battery thermal runaway behavior, J. Hazard. Mater. 369 (2019) 268–278, https://doi.org/10.1016/j.jhazmat.2019.01.049.
[6] M. Chen, O. Dongxu, S. Cao, J. Liu, Z. Wang, J. Wang, Effects of heat treatment and SOC on fire behaviors of lithium-ion batteries pack, J. Therm. Anal. Calorim. 136 (2019) 2429–2437, https://doi.org/10.1007/S10973-018-7864-9.
[7] M.N. Richard, J.R. Dahn, Accelerating rate calorimetry study on the thermal stability of lithium intercalated graphite in electrolyte. I. Experimental, J. Electrochem. Soc. 146 (1999) 2068–2077, https://doi.org/10.1149/1.1391893.

[8] G. Venugopal, Characterization of thermal cut-off mechanisms in prismatic lithium-ion batteries, J. Power Sources 101 (2001) 231–237, https://doi.org/10.1016/S0378-7753(01)00782-0.
[9] X. Feng, M. Fang, X. He, M. Ouyang, L. Lu, H. Wang, M. Zhang, Thermal runaway features of large format prismatic lithium ion battery using extended volume accelerating rate calorimetry, J. Power Sources 255 (2014) 294–301, https://doi.org/10.1016/j.jpowsour.2014.01.005.
[10] P. Ping, Q. Wang, P. Huang, J. Sun, C. Chen, Thermal behaviour analysis of lithium-ion battery at elevated temperature using deconvolution method, Appl. Energy 129 (2014) 261–273, https://doi.org/10.1016/j.apenergy.2014.04.092.
[11] B. Mao, H. Chen, Z. Cui, T. Wu, Q. Wang, Failure mechanism of the lithium ion battery during nail penetration, Int. J. Heat Mass Tran. 122 (2018) 1103–1115, https://doi.org/10.1016/j.ijheatmasstransfer.2018.02.036.
[12] X. Feng, X. He, M. Ouyang, L. Lu, P. Wu, C. Kulp, S. Prasser, Thermal runaway propagation model for designing a safer battery pack with 25Ah LiNixCoyMnzO2 large format lithium ion battery, Appl. Energy 154 (2015) 74–91, https://doi.org/10.1016/j.apenergy.2015.04.118.
[13] H. Wang, A. Tang, K. Huang, Oxygen evolution in overcharged LixNi1/3Co 1/3Mn1/3O2 electrode and its thermal analysis kinetics, Chin. J. Chem. 29 (2011) 1583–1588, https://doi.org/10.1002/CJOC.201180284.
[14] C. Essl, A.W. Golubkov, A. Fuchs, Comparing different thermal runaway triggers for two automotive lithium-ion battery cell types, J. Electrochem. Soc. 167 (2020) 130542, https://doi.org/10.1149/1945-7111/ABBE5A.
[15] P. Röder, N. Baba, H.D. Wiemhöfer, A detailed thermal study of a Li[Ni0.33Co0.33Mn 0.33]O2/LiMn2O4-based lithium ion cell by accelerating rate and differential scanning calorimetry, J. Power Sources 248 (2014) 978–987, https://doi.org/10.1016/j.jpowsour.2013.09.146.
[16] D.D. MacNeil, J.R. Dahn, The reaction of charged cathodes with nonaqueous solvents and electrolytes: I. Li[sub 0.5]CoO[sub 2], J. Electrochem. Soc. 148 (2001) A1205, https://doi.org/10.1149/1.1407245.
[17] C. Lin, H. Yan, C. Qi, J. Mao, L. Lao, Y. Sun, T. Ma, D. Liu, Research on thermal runaway and gas generation characteristics of NCM811 high energy density lithium-ion batteries under different triggering methods, Case Stud. Therm. Eng. 64 (2024) 105417, https://doi.org/10.1016/J.CSITE.2024.105417.
[18] M. Chen, D. Ouyang, J. Weng, J. Liu, J. Wang, Environmental pressure effects on thermal runaway and fire behaviors of lithium-ion battery with different cathodes and state of charge, Process Saf. Environ. Prot. 130 (2019) 250–256, https://doi.org/10.1016/J.PSEP.2019.08.023.
[19] L. Yi, Y. Dong-xing, Z. Shao-yu, H. Qun-ming, L. Xin, W. Jian-qiang, T.F.R. Institute, On the fire extinguishing tests of typical lithium-ion battery, J. Saf. Environ. (2015) 120–125.
[20] J. Xu, Q. Duan, L. Zhang, Y. Liu, C. Zhao, Q. Wang, Experimental study of the cooling effect of water mist on 18650 lithium-ion battery at different initial temperatures, Process Saf. Environ. Prot. 157 (2022) 156–166, https://doi.org/10.1016/j.psep.2021.10.034.
[21] L. Zhang, Y. Li, Q. Duan, M. Chen, J. Xu, C. Zhao, J. Sun, Q. Wang, Experimental study on the synergistic effect of gas extinguishing agents and water mist on suppressing lithium-ion battery fires, J. Energy Storage 32 (2020), https://doi.org/10.1016/J.EST.2020.101801.
[22] W. Peng, Y. Zhang, S. Zhang, X. Liu, Experimental study on the inhibition effect of water mist containing additives on the thermal runaway of lithium battery, Process Saf. Environ. Prot. 182 (2024) 999–1007, https://doi.org/10.1016/j.psep.2023.12.047.
[23] C. Edison, Considerations for ESS Fire Safety, DNV GL, Oslo, Norway, 2017. (Accessed 3 May 2025).
[24] J. Xu, P. Guo, Q. Duan, X. Yu, L. Zhang, Y. Liu, Q. Wang, Experimental study of the effectiveness of three kinds of extinguishing agents on suppressing lithium-ion battery fires, Appl. Therm. Eng. 171 (2020), https://doi.org/10.1016/j.applthermaleng.2020.115076.
[25] L. Zhang, F. Ye, Y. Li, M. Chen, X. Meng, J. Xu, J. Sun, Q. Wang, Experimental study on the efficiency of Dodecafluoro-2-Methylpentan-3-One on suppressing large-scale battery module fire, Fire Technol. 59 (2023) 1247–1267, https://doi.org/10.1007/S10694-022-01322-2.
[26] Y. Liu, K. Yang, M. Zhang, S. Li, F. Gao, Q. Duan, J. Sun, Q. Wang, The efficiency and toxicity of dodecafluoro-2-methylpentan-3-one in suppressing lithium-ion battery fire, J. Energy Chem. 65 (2022) 532–540, https://doi.org/10.1016/J.JECHEM.2021.05.043.
[27] Z. Huang, P. Liu, Q. Duan, C. Zhao, Q. Wang, Experimental investigation on the cooling and suppression effects of liquid nitrogen on the thermal runaway of lithium ion battery, J. Power Sources 495 (2021), https://doi.org/10.1016/j.jpowsour.2021.229795.
[28] R. Hui, Luoxiao-feng, L. An, W. Zhi-hong, X. Qing-qing, Z. Zheng, Study on comparative fire extinguishing tests between ternary lithium battery cabin and Lithium iron phosphate battery cabin of electric ships, Fire Sci. Technol. 40 (2021) 433. https://www.xfkj.com.cn/EN/. (Accessed 3 May 2025).